Published in final edited form as:

Bioelectrochemistry. 2015 December ; 106(Pt A): 141–149. doi:10.1016/j.bioelechem.2015.05.002.

Surface Chemistry Enhanced Microbial Bioelectrocatalysis

Carlo Santoro[a,b,1], **Sofia Babanova**[a,1], **Kateryna Artyushkova**[a], **Jose' A. Cornejo**[a], **Linnea Ista**[c], **Orianna Bretschger**[d], **Enrico Marsili**[e], **Plamen Atanassov**[a,*], and **Andrew J. Schuler**[b,**]

[a]Department of Chemical & Nuclear Engineering, Center for Emerging Energy Technologies, University of New Mexico, Albuquerque, NM 87131, USA

[b]Department of Civil Engineering, University of New Mexico, Albuquerque, NM 87131, USA

[c]Center of Biochemical Engineering, University of New Mexico, Albuquerque, NM 87131, USA

[d]J. Craig Venter Institute, 4120 Torrey Pines Road, San Diego, CA 92037, United States

[e]Singapore Centre on Environmental Life Sciences Engineering (SCELSE), Nanyang Technological University, 60 Nanyang Drive, 637551 Singapore, Singapore

Abstract

Self-assembled monolayers (SAMs) modified gold anodes are used in single chamber microbial fuel cells (SCMFC) for organics removal and electricity generation. Hydrophilic ($-N(CH_3)_3^+$, −OH, −COOH) and hydrophobic ($-CH_3$) SAMs are examined for their effect on bacterial attachment, current and power output. The different substratum chemistry affects both the current and power output and the community composition of the electrochemically active biofilm formed. Of the four SAM-modified anode tested, $-N(CH_3)_3^+$ results in shortest start up time, highest single electrode polarization and power density, followed by −OH and –COOH SAMs. Hydrophobic SAM decreases bacteria attachment and anodes performance in comparison to hydrophilic SAMs. Electron transfer rate is faster on the $N(CH_3)_3^+$-surface than on other surfaces, and correlates with a high abundance of *δ-Proteobacteria*, including electrochemically active species. A consortium of *Clostridia* and *δ-Proteobacteria* is found on all the anode surfaces, suggesting a synergistic cooperation under anodic conditions.

Keywords

microbial fuel cells; self assembled monolayer; surface modification; bioelectrocatalysis; anode biofilm analysis

[*]Corresponding authors: Prof. Plamen Atanassov. Department of Chemical and Nuclear Engineering, University of New Mexico, MSC01 1120, Farris Engineering Center 247, 1 University of New Mexico, Albuquerque 87101-0001, United States. Tel.: +1 505 277 6112. ; Email: plamen@unm.edu (P. Atanassov) [**]Prof. Andrew. J. Schuler. Department of Civil Engineering, University of New Mexico. MSC01 1070, University of New Mexico, Albuquerque, New Mexico 87131-0001, United States. Tel.: +1 (505) 277 4556. ; Email: schuler@unm.edu (A.J. Schuler)

[1]the two authors have contributed equally to the manuscript

Introduction

Numerous bacterial species have shown the ability to oxidize organic compounds and use insoluble metal oxides and electrodes as their terminal electron acceptor. [1–4]. Extracellular electron transfer in bacteria enable the construction and operation of bioelectrochemical systems called microbial fuel cells (MFCs) [5].

The rate limiting step in MFC operation is the electron transfer rate at the biofilm/electrode interface, which determines the maximum current and power output under steady state conditions. Therefore, it is critical to optimize the electrode morphology and chemistry to promote fast electron transfer rate. This goal can be achieved through selection of specific electrode materials, enrichment with anode-respiring bacteria, morphological or chemical modifications of electrode surface [5–7]. The electrode material and morphology should facilitate bacterial attachment and subsequent biofilm formation. At the same time, anode surface chemistry along with the biofilm formation should enhance electron transfer from bacteria to the electrode [8–10]. Several thermal or chemical treatments have been described to reduce MFC start-up time by facilitating rapid cell attachment and biofilm development for enhanced power output in MFC [5, 11–12]. Thermal treatment of the electrodes leads to modification of the surface roughness and porosity and thus enhances cells concentration and biofilm development [13–16]. Depending on the gas atmosphere (e.g., nitrogen, oxygen, ammonia, etc.) used in thermal treatment, hydrophilic functional groups can be added on the electrode surface [17]. The main purpose of the chemical treatment is to introduce functional groups (typically nitrogen and oxygen containing groups) that improve cell attachment and biofilm development on electrode surface [18–21]. Several compounds, such as nitric acid [18,19], ethylenediamine [18], ammonium nitrate [19], ammonium persulfate [19], polyaniline [20], 4(N,N-dimethylamino)benzene diazonium [21] have been used for surface chemical modification of carbonaceous electrodes. However, as previously shown [22], the chemical treatment of carbonaceous surfaces (e.g., carbon cloth) affect both the chemistry and morphology (e.g., roughness and porosity) of said surfaces, thus a clear discrimination of the benefits provided by chemical and surface effects is not straightforward. [22]. The inability to distinguish the influence of only one parameter from the whole set of parameters that are usually altered through the commonly used surface modification techniques is a result of the intercorrelation between the introduced variances in the parameters' magnitudes [23]. Therefore, the impact of the anode surface chemistry on current and power output in MFC should be studied using flat electrode material, thus de-coupling chemical effects from change in surface morphology.

Recently, Guo et al. [10] studied the influence of the surface charge and hydrophobicity on the current output of anodes operated in half-cell bioelectrochemical systems. They modified glassy carbon electrodes through electrochemical grafting with aryl dyazonium salts. As a result, the surface of each anode has been altered distinctively to be hydrophilic (−OH, SO_3^-, $-N(CH_3)_3^+$) or hydrophobic ($-CH_3$) with positive, negative or neutral charge [10]. All anodes were immersed in the same electrochemical cell with the identical electrolyte and polarized at the constant potential (−0.2 V vs Ag/AgCl (3.5 M KCl)). Higher biomass attachment was measured on hydrophilic and positively charged surfaces, which was directly related to the current output [10]. The microbial biofilm on the best performing anodes was

enriched in electrochemically active microorganisms (e.g., *Geobacter* sp). The same conclusion has been reported by Picot et al., who also observed significant increases in anode current output when the surface was amended with positively charged phenylphosphanium cations [24].

While these studies have added new knowledge relative to how anode surface modifications improve current and power output, the specific effects of given functional groups on MFC startup time, current and power output are still not well understood. In this study, ω-substituted alkanethiolates on gold terminated with functional groups ($-N(CH_3)_3^+$, −COO−, −OH and $-CH_3$) are used for the modification of gold anodes. We have previously shown that SAMs improve cells attachment and early biofilm formation and extend this model surface to electrochemical studies. [25–28]. Here, SCMFC equipped with activated carbon air cathodes are used. The correlation between the surface chemistry of the anode and the SCMFC current and power output is investigated. SAMs-modified gold electrodes are employed as anodes to eliminate the morphology effects associated with conventional carbonaceous electrode. Separate SCMFC are used for each anode material, to avoid undesired shunt-current losses or interaction among the different electrodes exposed to the same solution. Following electrochemical characterization for 45 days, DNA from anodic biofilms is sequenced to characterize the electrogenic communities and identify any phylogenetic differences that might have occurred as a function of the unique surface modifications.

2. Materials and Method

2.1 Self Assembled-Monolayer production

Microscope glass coverslips (24 × 60 mm, #1, VWR, USA) were cleaned under UV ozone. The vacuum chamber was evacuated to $\sim 10^{-6}$ millitorr and a 15 Å Cr layer was deposited followed by 300 Å gold. Immediately after gold deposition, samples were incubated in 1 mM ethanolic solutions of 1-mercaptoundecanol (OH; Aldrich, St. Louis MO), undecanethiol (CH_3; Aldrich, St. Louis, MO),1-mercaptoundecanoic acid (COOH, Aldrich, St Louis, MO) 1-mercaptoundecyl trimethylamine ($N(CH_3)_3^+$; Prochimia, Poland) [25–31].

2.2 MFC Configuration and cathode material

Single chamber microbial fuel cells (SCMFC) with a volume of 130 mL were assemblied as previously described [32]. The anolyte was 50% 0.1 M phosphate buffer solution (PBS) with 0.1 M KCl and 50% of activated sludge from the Albuquerque Wastewater Treatment Plant. Sodium acetate ($C_2H_3NaO_2$, 5 g L^{-1}) was used as a substrate and introduced periodically in each MFC to maintain non-limiting substrate concentration. The pH of the anolyte was 7.4–7.5 and remained constant along the entire experiment [22]. SAM-modified gold anodes (geometric area 14.4 cm^2) were assembled with two coverslips using a titanium wire with the functionalized surface facing the medium solution. The anode was connected to the cathode through an external resistance of 1000 Ω. The cathode used in this work has been previously described [33]. Briefly, activated carbon (Calgon, USA) with a surface area of 802 m^2 g^{-1} was grinded with 20% wt PTFE (60% dispersion in water, Sigma Aldrich). 60±2 mg cm^{-2} of the obtained mixture were pressed at 1400 psi for 2 minutes on a carbon cloth

(30% wt wet proof, Fuel Cell Earth) used as the electron collector. The cathode assembly was then heated at 200 °C for 1 h before utilization. The cathode had a geometric surface area of 3.5 cm^2 directly exposed to the electrolyte. The SMFCs were operated in duplicate for each SAM-modified anode material at room temperature (21±1°C).

2.3 Electrochemical measurements

The overall SCMFC potential was recorded every 25 min using a datalog system (Personal DAQ/56, USA) connected to a PC for over 45 days. At the end of the experiment, anode and cathode potentiodynamic polarization curves were taken using a three-electrode configuration as previously described using a VersaStat potentiostat (Princeton Applied Research, USA) [34]. Briefly, the electrode under investigation (anode or cathode) was used as the working electrode, Ag/AgCl 3M (+0.21 V vs. SHE) was used as the reference electrode and a SS A316 mesh with the same area of the working electrode was used as a counter electrode. The anode potential was scanned from open circuit potential (OCP) to 0 V vs Ag/AgCl 3M. The cathode potential was scanned from OCP to −0.3 V vs Ag/AgCl 3M. The scan rate utilized for the potentiodynamic curve was 0.2 and −0.2 mV s^{-1}, respectively [35]. The SCMFC cell polarization curves were carried out after the single electrode polarizations in two electrode mode, connecting the anode as working and the cathode as counter and reference electrode. The polarization was started after the OCP stabilized (approximately one hour), and then the polarization curve was measured from the open circuit cell potential (OCP) to 0.01 V (vs Ag/AgCl 3M). The power (P) was obtained using the Ohm's law P = E × I where E and I are the SCMFC potential and current, respectively. Power and current are normalized to the anode geometric surface area (14.4 cm^2).

2.4 Electron transfer rate evaluation

After the 45 day MFC operation under constant load, cyclic voltammetries (CVs) of the four SAM-modified gold electrodes were carried out at various scan rates (2 to 200 mV s^{-1}). A linear dependence between the peak currents and the scan rate of the CV indicated surface confined electrochemical reaction [36]. Laviron plots [37] were used to evaluate the electron transfer rate constant (K_{ET}) on the modified gold surfaces, according to the equation:

$$\eta = \frac{2.3 * \mathrm{RT}}{n\alpha F} \log \nu \text{ or } K_{ET} = \frac{n * \alpha * \nu * F}{2.3 * \mathrm{RT}}$$

where η is the reaction overpotential (V), ν is the scan rate of the CV (V s^{-1}), n is the number of electrons (assumed to be one since we suppose that the peaks are associated with cytochromes electrochemical transformation), α is the charge transfer coefficient, R is the universal gas constant, F is the Faradaic constant and T is the temperature in K.

2.5 Biofilm characterization on the electrode

At the end of the 45 days experiments, anodic and cathodic biofilm were removed by scraping out the electrodes. Pyrosequencing was done on one anode per each electrode material and on the planktonic biomass of the SCMFC equipped with $N(CH_3)_3^+$–modified anode. DNA was extracted using sucrose lysis/cetyltrimethylammonium bromide (CTAB) as previously described [38], and its purity was evaluated from the ratio of absorbances at 260

and 280 nm. Samples were shipped on ice for DNA pyrosequencing by Research and Testing Laboratories (Lubbock, TX, USA). Bacterial tag-encoded FLX amplicon pyrosequencing was performed as described previously [39] with small modifications to utilize the Titanium sequencing platform (Roche Applied Science, Indianapolis, IN). A single 35 cycle PCR step with Qiagen HotStar master mix and addition of 0.5 U of HotStar HiFidelity polymerase were used in each reaction (Qiagen, Valencia, CA). The primers were 28f (5'-GAG TTT GAT CNT GGC TCA G-3') and 519r (5'-GTN TTA CNG CGG CKG CTG-3') (*Escherichia coli* 16S gene numbering). Pyrosequence reads were analyzed at UNM using AmpliconNoise 1.25 [40] to remove low quality sequences, which included sequences less than 200 bp in length, with an average quality score of less than 25, containing ambiguous characters, and/or without the correct primer sequence. A workflow script in QIIME 1.80 was used to pick operational taxonomic units (OTUs) at the 97% sequence identity level. Representative sequences from each OTU were identified by the Ribosomal Database Project44 classification method using QIIME, with assignment of taxonomic identities using the Greengenes 16s rRNA gene database [41].

3. Results and Discussion

Gold electrodes were modified with self assembled monolayers (SAMs) having four different terminal groups, $–CH_3$, −OH, −COOH and $−N(CH_3)_3^+$. A stable molecular monolayer coated uniformly the surface as showed previously [31]. As the aim of this study was to compare the influence of the surface chemistry on biofilm formation and current generation in MFC rather than compare modified vs. unmodified anodes, no control experiment with bare gold electrode was carried out.

3.1 SCMFC potential

The SCMFC potential under constant external load (1000 Ω) was monitored for 45 days (Figure 1). As in many other MFC studies, the potential increased with time, indicating electrochemically active biofilm formation. However, the potential evolution with time was different for each material, indicating differences in electroactivity and electron transfer rate [42].

MFCs fitted with $−N(CH_3)_3^+$–SAM anodes showed a rapid potential increase (after 15 d), followed by –COOH (17 d), $−CH_3$ (17 d) and –OH (20 d) (Figure 1). The $−N(CH_3)_3^+$-MFCs showed the fastest potential slope (170–195 mV d^{-1}) and achieved stable conditions after roughly 18 days. COOH−MFCs showed a slower potential slope (75–96 mV d^{-1}) and stabilized after 22–23 days. The potential slope of OH-MFCs could be divided in two different parts: i) at potential < 0.15 V, the slope was of 21–25 mV day^{-1}; ii) at potential 0.42 > E > 0.15 V with the slope increased to 50–56 mV day^{-1}. Finally, the E slope of CH_3-MFCs was much smaller than the other materials, only 2.2–2.3 mV day^{-1}. These results show that anode coating affect both the start-up time of potential production and the rate of potential increase with time, which in turn correlate to the attachment and growth of electrochemically active biofilms.

Despite the different start-up times, the $N(CH_3)_3^+$−, COOH− and OH-MFCs reached a similar stable voltage output (0.41–0.43 V), as the external resistance chosen was higher

than the smaller sustainable resistance [43]. However, the potential of CH_3-MFC increased slowly over time and stabilized after 40 days to 0.06 V (Figure 1).

3.2 Anode polarization curves

To study the anode behavior independently of the cathode, the anode electrochemical response was measured using potentiodynamic polarization curves after 45 days of constant MFCs operation (Figure 2). Despite the fact that the voltage achieved at 1000 Ω external resistance after day 45 of MFCs polarization was approximately the same for $N(CH_3)_3^+$−, COOH− and OH-MFCs, the different surface chemistry of the anodes results in a different anodic polarization behavior. Maximum current densities of 225–230 μA cm^{-2} were achieved by the $-N(CH_3)_3^+$ modified anodes at approximately −0.40 V vs. Ag/AgCl. The peak observed at −0.40 V is likely due to direct electron transfer at the interface biofilm/electrode, as evidenced by the scan rate analysis (Figure 5.a). The same peak was observed in the polarization curves of all anodes studied except the CH_3-modified one. The $-N(CH_3)_3^+$-anode demonstrated another peak at higher anodic potential (−0.27 V vs. Ag/AgCl). The maximum current densities achieved for each SAMs-modified anode follow the same trends as the voltage startup conditions in that the $-N(CH_3)_3^+$ systems showed the highest performance followed by −COOH, −OH and $-CH_3$, respectively (Figure 2).

The $-N(CH_3)_3^+$-MFCs showed the highest anode current densities and shortest start up time most likely due to bacteria preference towards hydrophilic and positively charged surfaces in agreement with previous studies [10].

We have previously demonstrated that different bacteria exhibit different attachment responses to SAMs [25, 27, 31]. −COOH and −OH- SAM generated much lower current densities relative to the $N(CH_3)_3^+$-anodes. These data suggest that the surface chemistry directly affect biofilm formation and/or specific biofilm function. Further, the −COOH, −OH and $-CH_3$-modified surfaces may limit biofilm production or electron transfer rate [10]. Cathode polarization curves (not shown) resulted in similar trends for each system and indicated that the cathode electrochemical performance was not the rate limiting factor.

3.3 MFC polarization curves and power generation

The $N(CH_3)_3^+$−, COOH− and OH-MFCs had similar OCV values at 550–565 mV and similar initial current output till roughly 70 μA cm^{-2} (Figure 3.a). As the current densities increase, the IE curves showed diffusion limitations going into overshoot conditions [44]. Particularly, the OH-MFCs showed mass transfer control at roughly 70 μA cm^{-2} while the COOH−MFCs showed diffusion limitations at roughly 125 μA cm^{-2} and the $N(CH_3)_3^+$−MFC was limited by mass transfer at roughly 200 μA cm^{-2}.

The MFCs with $–CH_3$ modified anodes had significantly lower OCPs (450 mV) and significantly lower short circuit currents of 5–7 μA cm^{-2}. The $N(CH_3)_3^+$-MFCs had a maximum power density of 40–41 μW cm^{-2} followed by COOH−MFC with 35–37 μW cm^{-2} and by OH-MFCs with 25–28 μW cm^{-2}. The CH_3-MFCs had the lowest performances with a P_{max} of only 1.2 μW cm^{-2} (Figure 3.b). Comparison between Figure 2 and Figure 3 shows that MFC polarization measurements followed the same trends of the anode polarization curves.

3.4 Cyclic voltammetry

Cyclic voltammetry (CV) measurements of the different SAMs-modified anodes were carried out at various scan rates (2 – 200 mV s^{-1}) under identical conditions after 45 days. At 2 mV s^{-1}, the turnover curve onset was at −0.490 V vs. Ag/AgCl for the −COOH and the $-N(CH_3)_3^+$, but was poorly defined for the OH and CH_3 modified electrodes (Figure 4). This result indicate that extracellular electron transfer to the electrode was faster at the −COOH and the $-N(CH_3)_3^+$ modified electrodes. The voltammetry roughly correlate with the phylogenetic analysis, in what the −COOH and the $-N(CH_3)_3^+$ electrodes have the highest concentration of *δ-Proteobacteria*. A further redox species oxidize irreversibly at −180 to −110 mV and do not result in turnover electron transfer (Figure 4).

Although the shape of the CVs of the $N(CH_3)_3^+$ and COOH microbial anodes is similar to the cyclic voltammetry of *Geobacter sulfurreducens* [10,45,46], no *Geobacter* species were revealed when the anodes biofilms were subjected to pyrosequencing (see the section below). This may indicate that different electrochemically active bacteria posses similar electrochemical features and behavior in terms of identical outer membrane redox carriers and electron-transfer mechanisms as it has been proposed by Lui et al. and Ishii et al. [46–48]. A linear dependence was observed when the peaks of current at the various scan rates were plotted versus the cyclic voltammetry scan rate (Figure 5.a), which indicates surface confined electrochemical reactions and allowed the utilization of Laviron plots (Figure 5.b) to evaluate the electron transfer rate constant on the modified gold surfaces. Laviron plot results suggest that direct electron transfer is the predominant mode of electron transfer in all MFC analyzed and the turnover curve may be attributed to outer membrane cytochrome involved in the electron transfer at the biofilm/electrode interface. For the evaluation of the K_{ET}, the following peaks were taken into account: i) for $-N(CH_3)_3^+$ enriched surfaces the oxidation and reduction peaks at −0.380 and −0.445 V vs. Ag/AgCl, respectively were used for the calculation; ii) for COOH−anodes, the peaks were: oxidation peak at −0.370 V and reduction peak at −0.440 V vs. Ag/AgCl; iii) for the –OH modified anodes the peaks were: oxidation peak at −0.425 V and the reduction at −0.515 V vs. Ag/AgCl; and iv) for CH_3-sample the peaks used are the only one showing up on the CV, −0.520 V vs. Ag/AgCl (reduction peak) and −0.175 V vs. Ag/AgCl (oxidation peak).

The results for the K_{ET} along with the formal redox potential of the redox reactions are shown in Table 1.

The electron transfer rate constant of the evaluated redox reaction for $-N(CH_3)_3$, −COOH and −OH modified gold surfaces had the same order of magnitude, which was significantly higher than the K_{ET} calculated for the $-CH_3$ anodes. This contributes to the significant difference in the generated current and power densities between the $-N(CH_3)_3^+$, −COOH, −OH and the $-CH_3$-anodes.

The logarithmic dependence of the current from the K_{ET} (Figure 6) suggests that the rate of the electron transfer is not the main factor determining the MFCs current and power output. No clear trend between the formal redox potential of the reaction and the MFCs current was observed.

3.5 Anodic and cathodic biofilm analysis

Pyrosequencing of 16S rRNA gene amplicons derived from the anode-associated biomass shows diverse bacterial populations at the anode surfaces (Figure 7). A phylum-level analysis (Figure 7.a) indicates that phylum *Proteobacteria* comprised between 32 % and 37 % of the anode-associated biofilms. Specifically, the $-N(CH_3)_3^+$ modified surface featured *Proteobacteria* in a relative abundance of 36 %, the −COOH had 37 % relative abundance, and −OH had 32 % relative abundance. The $-N(CH_3)_3^+$ bulk solution (labeled as WW in Figure 7) also showed 37 % relative abundance of *Proteobacteria*. However, *Proteobacteria* only comprised occupied approximately 6 % of the biofilm associated with the $–CH_3$ modified anode.

The phylum *Firmicutes* had a high relative abundance in all of the communities, between 21 % and 34 % of the biofilm. The biofilm associated with the $-CH_3$-modified electrode had the highest relative abundance of *Firmicutes* at 34 %. Interestingly, *Firmicutes* have been identified in many different microbial fuel cell reports, including a particular strain (*Firmicutes Thermincola* sp. strain JR) that was isolated from thermophilic microbial fuel cells and was able to directly transfer electrons to an anode surface [49].

The phylum *Bacteroidetes* was present in all of the communities with relative community abundance of 22 % ($-N(CH_3)_3^+$), 12 % (−COOH), 6 % (−OH), 13 % ($-CH_3$) and 15 % (WW). The $-CH_3$ modified anode also had a relatively high abundance of phyla *Lentisphaerae* (24 %) and *Actinobacteria* (19 %) as compared to the other samples.

The class-level analysis of the anode communities shows that the phylum *Proteobacteria* featured class *δ-Proteobacteria, β-Proteobacteria, γ-Proteobacteria, ε-Proteobacteria* and *α-Proteobacteria*. Class *δ-Proteobacteria* had the highest relative abundance in the $-N(CH_3)_3^+$, −COOH and −OH anode biofilms, and very low relative abundance in the $-CH_3$ anode-associated biofilm and the $-N(CH_3)_3^+$ bulk solution (WW). Several members of class *δ-Proteobacteria* and *γ-Proteobacteria* have been reported as electrochemically active microbes in bioelectrochemical systems [47, 48, 50–56].

The high relative abundance of class *δ-Proteobacteria* in all of the biofilms that showed good current and power output ($-N(CH_3)_3^+$, −COOH and −OH), suggests that these community members are active in electron transfer to the anode surfaces. The −COOH anode-associated biofilm and the WW also featured a small percentage of class *γ-Proteobacteria*, which suggests that these community members might be active in multiple functions, including electron transfer to the anode and possibly fermentation of complex substrates in the bulk solution.

The presence of class *β-Proteobacteria* in wastewater-enriched microbial fuel cells has also been reported by several MFC researchers [47–48, 50–51]; however, the functional role(s) of these microbes have not been comprehensively defined, and members of this class may perform multiple functions within the biofilm.

Interestingly, all the reactors featured a high relative abundance of fermentative microbes including class *Clostridia, Bacterioidia, Deferribacteres* and *Lentisphaerea*. This result

suggests that acetate was not the sole carbon source for the community and that residual complex carbon substrates from the activated sludge inoculum may also have been used as electron donors for the biofilm and planktonic communities. Members of class *Clostridia*, *Bacterioidia*, *Deferribacteres* and *Lentisphaerea* have been reported in several wastewater-enriched microbial fuel cells [47,48, 50–55, 57,58], and it is speculated that these organisms are critical for converting sugars and other complex substrates to simple volatile fatty acids that are the preferred carbons sources for electrochemically active δ- and γ-*Proteobacteria* .

A more detailed sequencing effort is required to identify strain-level associations with the various electrode surface chemistries; however, the class-level analysis suggests that there may have been different community members contributing to electron transfer at the various chemically-modified surfaces. The results strongly suggest that the surface chemistry (charge and hydrophobicity) of the $-CH_3$-modified anode had the most effect on microbial taxonomic enrichment, which negatively impacted the overall system function. The lack of δ-*Proteobacteria* members and a higher relative abundance of diverse fermentative members (e.g. *Bacilli*, *Lentisphaerae* and *Actinobacteria*) correlates with the low electrochemical performance of the $-CH_3$-modified system, and suggests that fermentation was the primary function of this community.

3.6 Relationship between electrochemical output and anodic microbial community

Surface modifications of the anode change the hydrophilicity, surface charge, surface tension, and the morphology of the electrode, particularly when carbonaceous electrodes are used. [10, 22, 59]. The hydrophilicity of the anode increased when the gold surface was modified with −OH, −COOH and $-N(CH_3)_3^+$ SAMs and decreased with the $-CH_3$ SAM. Previously reported contact angles measurements in ultrapure water showed similar values (22–23°) for −OH, −COOH and $-N(CH_3)_3^+$ SAMs despite differently surface charges while $-CH_3$ SAM had a much higher values (118±1°), which is typical for hydrophobic surfaces [31]. The increased surface hydrophilicity facilitates bacteria attachment and biofilm development [10]. The positive charge of $N(CH_3)_3^+$ group further facilitate attachment of negatively charged bacteria at circumneutral pH. Therefore, start-up time followed the order: $-N(CH_3)_3^+ < -COOH < -OH < -CH_3$. Depending on the pH, negatively charged surface groups, such as $-COO^-$ introduces repulsion forces between the modified electrode surface and bacteria and thus hinders bacteria attachment and biofilm formation [24]. Lower bacterial density on −COOH containing anodes was also observed by Tanh et al. [60]. At the pH of wastewater used in this study, it is not entirely clear if the −COOH group from the $SH(CH_2)_{10}COOH$ is deprotonated or not. The $pK_{1/2}$ of $HS(CH_2)_{10}COOH$ has been found to be 7.4 and the pH of the electrolyte in this study was 7.4–7.5. Sumner et al. suggested that the carboxylic acid terminus of SAMs can interact with the peptide bonds in proteins via strong hydrogen bonds [61]. Thus, −COOH could bind outer membrane cyctochromes, which are responsible for electron transfer in model electrochemically active microorganisms. The same authors also showed that, despite the low attached cell concentration on $-CH_3$ and −COOH terminated gold surface, the MFC current output was much higher when the gold surface was populated with carboxylic groups, because of the enhanced electronic coupling at the biofilm/electrode interface.

The electron transfer rate at the biofilm/electrode interface depends on the surface chemistry of the anodes, which affects bacterial attachment. The variations in the surface hydrophilicity and the charge of the modified electrode affect also the electrolyte-electrode interactions, as recently shown by Guo et al. [10], using a ferricyanide probe. In this study, we show that the highest K_{ET} occurs on the $-N(CH_3)_3^+$ surfaces, which contributes to the higher current and power output of these electrodes, along with their higher hydrophilicity and positive charge. Furthermore, $-N(CH_3)_3$ showed higher relative abundance of *δ-Proteobacteria*.

It is well-known that an increase in the relative abundance of *δ-Proteobacteria* in the bacterial biofilm [47, 48, 50–56] leads to enhancement of the anodes electrical output, as this bacterial class includes several electrochemically active species. However, due to the complexity of the carbon compounds in wastewater, a consortium between *Clostridia* and *δ-Proteobacteria* result in increased electrochemical performance of the SCMFCs

4. Conclusions

Hydrophilic/hydrophobic SAM-modified gold anodes, harboring positive or negative functional groups, determine the current and power output of SCMFCs. Electrochemically active microorganisms attach preferentially on hydrophilic and positively charged surfaces. In fact, $-N(CH_3)_3^+$ modified anodes showed the shortest start-up time, the highest current and power densities and the fastest electron transfer rates among the materials investigated. Pyrosequencing showed the highest percentage of *δ-Proteobacteria* on $-N(CH_3)_3^+$ modified anodes, most likely responsible for direct electron transfer at the biofilm/electrode interface. A consortium of *Clostridia* and *δ-Proteobacteria* was found on all anode surfaces, suggesting synergistic effect, which warrants further investigation.

Acknowledgments

This project is funded by the Army Research Office Award W911NF-12-1-0208

References

1. Lovley DR. Bug juice: harvesting electricity with microorganisms. Nature Rev. Microbiol. 2006; 4:497–508. [PubMed: 16778836]
2. Torres CI, Marcus AK, Lee H-S, Parameswaran P, Krajmalnik-Brown R, Rittmann BE. A kinetic perspective on extracellular electron transfer by anode-respiring bacteria. FEMS Microbiol. Rev. 2010; 34:3–17. [PubMed: 19895647]
3. Bond DR, Strycharz-Glaven SM, Tender LM, Torres CI. On electron transport through Geobacter biofilms. ChemSusChem. 2012; 5:1099–1105. [PubMed: 22615023]
4. Logan B. Exoelectrogenic bacteria that power microbial fuel cells. Nature Rev. Microbiol. 2009; 7:375–381. [PubMed: 19330018]
5. Rinaldi A, Mecheri B, Garavaglia V, Licoccia S, Di Nardo P, Traversa E. Engineering materials and biology to boost performance of microbial fuel cells: a critical review. Energy Environ. Sci. 2008; 1:417–429.
6. Franks AE, Nevin KP. Microbial Fuel Cells. A Current Review, Energies. 2010; 3:899–919.
7. Mohan SV, Velvizhi G, Modestra JA, Srikanth S. Microbial fuel cell: Critical factors regulating bio-catalyzed electrochemical process and recent advancements. Renew. Sust. Energ. Rev. 2014; 40:779–797.

8. Liu X-W, Chen J-J, Huang Y-X, Sun X-F, Sheng G-P, Li D-B, Xiong L, Zhang Y-Y, Zhao F, Yu H-Q. Experimental and Theoretical Demonstrations for the Mechanism behind Enhanced Microbial Electron Transfer by CNT Network. Sci. Rep. 2014; 4 Article number: 3732.
9. He YR, Xiao X, Li WW, Sheng GP, Yan FF, Yu HQ, Yuan H, Wu LJ. Enhanced electricity production from microbial fuel cells with plasma-modified carbon paper anode. Phys. Chem. Chem. Phys. 2012; 14:9966–9971. [PubMed: 22699925]
10. Guo K, Freguia S, Dennis P, Chen X, Donose B, Keller J, Gooding J, Rabaey K. Effects of Surface Charge and Hydrophobicity on Anodic Biofilm Formation, Community Composition, and Current Generation in Bioelectrochemical Systems. Environ. Sci. Technol. 2013; 47:7563–7570. [PubMed: 23745742]
11. Wei J, Liang P, Huang X. Recent progress in electrodes for microbial fuel cells. Biores. Technol. 2011; 102:9335–9344.
12. Zhou M, Chi M, Luo J, He H, Jin T. An overview of electrode materials in microbial fuel cells. J. Power Sources. 2011; 196:4427–4435.
13. Wang X, Cheng S, Feng Y, Merrill MD, Saito T, Logan BE. Use of Carbon Mesh Anodes and the Effect of Different Pretreatment Methods on Power Production in Microbial Fuel Cells. Environ. Sci. Technol. 2009; 43:6870–6874. [PubMed: 19764262]
14. Ketep SF, Bergel A, Calmet A, Erable B. Stainless Steel Foam increases the current produced by microbial bioanodes in bioelectrochemical systems. Energy Env. Sci. 2014; 7(5):1633–1637.
15. Karra U, Manickam SS, McCutcheon JR, Patel N, Li B. Power generation and organics removal from wastewater using activated carbon nanofiber (ACNF) microbial fuel cells (MFCs). Int. J. Hydrog. Energy. 2013; 38:1588–1597.
16. Manickam SS, Karra U, Huang L, Bui N-N, Li B, McCutcheon JR. Activated carbon nanofiber anodes for microbial fuel cells. Carbon. 2013; 53:19–28.
17. Cheng S, Logan BE. Ammonia treatment of carbon cloth anodes to enhance power generation of microbial fuel cells. Electrochem. Commun. 2007; 9:492–496.
18. Zhu N, Chen X, Zhang T, Wu P, Li P, Wu J. Improved performance of membrane free single-chamber air-cathode microbial fuel cells with nitric acid and ethylenediamine surface modified activated carbon fiber felt anodes. Biores. Technol. 2011; 102:422–426.
19. Zhou M, Chi M, Wang H, Jin T. Anode modification by electrochemical oxidation: a new practical method to improve the performance of microbial fuel cells. Biochem. Eng. J. 2012; 60:151–155.
20. Lai B, Tang X, Li H, Du Z, Liu X, Zhang Q. Power production enhancement with a polyaniline modified anode in microbial fuel cells. Biosens. Bioelectron. 2011; 28:373–377. [PubMed: 21820889]
21. Saito T, Mehanna M, Wang X, Cusick RD, Feng Y, Hickner MA, Logan BE. Effect of nitrogen addition on the performance of microbial fuel cell anodes. Biores. Technol. 2011; 102:395–398.
22. Li B, Zhou J, Zhou X, Wang X, Li B, Santoro C, Grattieri M, Babanova S, Artyushkova K, Atanassov P, Schuler AJ. Surface Modification of Microbial Fuel Cells Anodes: Approaches to Practical Design. Electrochim. Acta. 2014; 134:116–126.
23. Babanova S, Bretschger O, Roy JN, Cheung A, Artyushkova K, Atanassov P. Innovative Statistical Interpretation of Shewanella oneidensis Microbial Fuel Cells Data. Phys. Chem. Chem. Phys. 2014; 16:8956–8969. [PubMed: 24691574]
24. Picot M, Lapinsonniere L, Rothaballer M, Barriere F. Graphite anode surface modification with controlled reduction of specific aryl diazonium salts for improved microbial fuel cells power output. Biosens. Bioelectron. 2011; 28:181–188. [PubMed: 21803564]
25. Callow JA, Callow ME, Ista LK, Lopez GP, Chaudhury MK. The influence of surface energy on the wetting behaviour of the spore adhesive of the marine alga Ulva linza (synonym Enteromorpha linza). J. R. Soc. Interface. 2005; 2:319–325. [PubMed: 16849189]
26. Finlay JA, Callow ME, Ista LK, Lopez GP, Callow JA. The influence of surface wettability on the adhesion strength of spores of the green alga Enteromorpha and the diatom Amphora. Integr. Comp. Biol. 2002; 42:1116–1122. [PubMed: 21680395]
27. Ista LK, Callow ME, Finlay JA, Coleman SE, Nolasco AC, Callow JA, Lopez GP. Effect of substratum surface chemistry and surface energy on attachment of marine bacteria and algal spores. Appl. Environ. Microbiol. 2004; 70:4151–4158. [PubMed: 15240295]

28. Ista LK, Lopez GP. Thermodynamic analysis of marine bacterial attachment to OEG SAMs. Biointerphases. 2013; 8:24. [PubMed: 24706137]
29. Hou S, Burton EA, Simon KA, Blodgett D, Luk Y-Y, Ren D. Inhibition of Escherichia coli biofilm formation by self assembled monolayers of functional alkanethiols on gold. Appl. Environ. Microbiol. 2007; 73:4300–4307. [PubMed: 17483274]
30. Bain CD, Troughton EB, Tao Y-T, Evall J, Whitesides GM, Nuzzo RG. Formation of monolayer films by the spontaneous assembly of organic thiols from solution onto gold. J. Am. Chem. Soc. 1989; 111:321–335.
31. Khan MMT, Ista LK, Lopez GP, Schuler AJ. Experimental and theoretical examination of surface energy and adhesion of nitrifying and heterotrophic bacteria determined using self-assembled monolayers. Environ. Sci. Technol. 2011; 45:1055–1060. [PubMed: 21189005]
32. Santoro C, Ieropoulos I, Greenman J, Cristiani P, Vadas T, Mackay A, Li B. Power generation and contaminant removal in single chamber microbial fuel cells (SCMFCs) treating human urine. Int. J. Hydrog. Energy. 2013; 38:11543–11551.
33. Santoro C, Artyushkova K, Babanova S, Atanassov P, Ieropoulos I, Grattieri M, Cristiani P, Trasatti S, Li B, Schuler AJ. Parameters characterization and optimization of activated carbon (AC) cathodes for microbial fuel cell application. Biores. Technol. 2014; 163:54–63.
34. Cristiani P, Carvalho ML, Guerrini E, Daghio M, Santoro C, Li B. Cathodic and anodic biofilms in single chamber microbial fuel cells. Bioelectrochem. 2013; 92:6–13.
35. Santoro C, Ieropoulos I, Greenman J, Cristiani P, Vadas T, Mackay A, Li B. Current generation in membraneless single chamber microbial fuel cells (MFCs) treating urine. J. Power Sources. 2013; 238:190–196.
36. Bard, A.; Faulkner, L. Electrochemical methods - Fundamentals and Applications. 2. John Wiley & Sons, Inc; 2001.
37. Laviron E. General expression of the linear potential sweep voltammetry in the case of diffusionless electrochemical systems. J. Electroanal. Chem. 1979; 101:19–28.
38. Mitchell KR, Takacs-Vesbach CD. A comparison of methods for total community DNA preservation and extraction from various thermal environments. J. Ind. Microbiol. Biot. 2008; 35:1139–1147.
39. Dowd SE, et al. Evaluation of the bacterial diversity in the feces of cattle using 16S rDNA bacterial tag-encoded FLX amplicon pyrosequencing (bTEFAP). Bmc Microbiol. 2008; 8:125. [PubMed: 18652685]
40. Quince C, Quince C, Lanzén A, Curtis TP, Davenport RJ, Hall N, Head IM, Read LF, Sloan WT. Accurate determination of microbial diversity from 454 pyrosequencing data. Nat. Methods. 2009; 6:639–641. [PubMed: 19668203]
41. McDonald D, Price MN, Goodrich J, Nawrocki EP, DeSantis TZ, Probst A, Andersen GL, Knight R, Hugenholtz P. An improved Greengenes taxonomy with explicit ranks for ecological and evolutionary analyses of bacteria and archaea. ISME J. 2012; 6:610–618. [PubMed: 22134646]
42. Rabaey K, Rodrıguez J, Blackall LL, Keller J, Gross P, Batstone D, Verstraete W, Nealson KH. Microbial ecology meets electrochemistry: electricity-driven and driving communities. ISME J. 2007; 1:9–18. [PubMed: 18043609]
43. Menicucci J, Beyenal H, Marsili E, Angathevar Veluchamy R, Demir G, Lewandowski Z. Procedure for determining maximum sustainable power generated by microbial fuel cells. Environ. Sci. Technol. 2006; 40:1062–1068. [PubMed: 16509358]
44. Winfield J, Ieropoulos I, Greenman J, Dennis J. The overshoot phenomenon as a function of internal resistance in microbial fuel cells. Bioelectrochem. 2011; 81:22–27.
45. Fricke K, Falk Harnisch, Schröder U. On the use of cyclic voltammetry for the study of anodic electron transfer in microbial fuel cells. Energy Env. Sci. 2008; 1:144–7.
46. Liu Y, Harnisch F, Fricke K, Schröder U. Improvement of the anodic bioelectrocatalytic activity of mixed culture biofilms by a simple consequitive electrochemical selection procedure. Biosens. Bioelectron. 2008; 24:1006–11. [PubMed: 18815023]
47. Ishii S, Suzuki S, Norden-Krichmar TM, Tenney A, Chain PSG, Scholz MB, Nealson KH, Bretschger O. A novel metatranscriptomic approach to identify gene expression dynamics during extracellular electron transfer. Nat. Commun. 2013; 4:1601. [PubMed: 23511466]

48. Ishii S, Suzuki S, Norden-Krichmar TM, Nealson KH, Sekiguchi Y, Gorby YA, Bretschger O. Functionally stable and phylogenetically diverse microbial enrichments from microbial fuel cells during wastewater treatment. PloS one. 2012; 7(2):e30495. [PubMed: 22347379]

49. Wrighton KC, Agbo P, Warnecke F, Weber KA, Brodie EL, DeSantis TZ, Hugenholtz P, Andersen GL, Coates JD. A novel ecological role of the Firmicutes identified in thermophilic microbial fuel cells. ISME J. 2008; 211:1146–1156. [PubMed: 18769460]

50. Ishii S, Suzuki S, Norden-Krichmar TM, Wu A, Yamanaka Y, Nealson KH, Bretschger O. Identifying the microbial communities and operational conditions for optimized wastewater treatment in microbial fuel cells. Water Res. 2013; 47(19):7120–7130. [PubMed: 24183402]

51. Ishii S, Suzuki S, Norden-Krichmar TM, Phan T, Wanger G, Nealson KH, Sekiguchi Y, Gorby YA, Bretschger O. Microbial population and functional dynamics associated with surface potential and carbon metabolism. ISME J. 2014; 8(5):963–978. [PubMed: 24351938]

52. Reguera G, McCarthy KD, Mehta T, Nicoll JS, Tuominen MT, Lovley DR. Extracellular electron transfer via microbial nanowires. Nature. 2005; 435(7045):1098–1101. [PubMed: 15973408]

53. Richter H, Lanthier M, Nevin KP, Lovley DR. Lack of electricity production by Pelobacter carbinolicus indicates that the capacity for Fe (III) oxide reduction does not necessarily confer electron transfer ability to fuel cell anodes. Appl. Environ. Microbiol. 2007; 16(73):5347–5353. [PubMed: 17574993]

54. Luo J, Yang J, He H, Jin T, Zhou L, Wang M, Zhou M. A new electrochemically active bacterium phylogenetically related to Tolumonas osonensis and power performance in MFCs. Biores. Technol. 2013; 139:141–148.

55. Jung S, Regan JM. Comparison of anode bacterial communities and performance in microbial fuel cells with different electron donors. Appl. Microbial. Biotechnol. 2007; 77(2):393–402.

56. Cristiani P, Franzetti A, Gandolfi I, Guerrini E, Bestetti G. Bacterial DGGE fingerprints of biofilms on electrodes of membraneless microbial fuel cells. Int. Biodeter. Biodegr. 2013; 84:211–219.

57. Zhang G, Zhao Q, Jiao Y, Wang K, Lee D-J, Ren N. Efficient electricity generation from sewage sludge using biocathode microbial fuel cell. Water Res. 2012; 46(1):43–52. [PubMed: 22078254]

58. Daghio M, Gandolfi I, Bestetti G, Franzetti A, Guerrini E, Cristiani P. Anodic and cathodic microbial communities in single chamber microbial fuel cells. N. Biotechnol. 2015; 32:79–84. [PubMed: 25291711]

59. Santoro C, Guilizzoni M, Correa Baena JP, Pasaogullari U, Casalegno A, Li B, Babanova S, Artyushkova K, Atanassov P. The effects of carbon electrode surface properties on bacteria attachment and start up time of microbial fuel cells. Carbon. 2014; 67:128–139.

60. Tang X, Guo K, Li H, Du Z, Tian J. Electrochemical treatment of graphite to enhance electron transfer from bacteria to electrodes. Biores. Technol. 2011; 102:3558–3560.

61. Crittenden SR, Sund CJ, Sumner JJ. Mediating Electron Transfer from Bacteria to a Gold Electrode via a Self-Assembled Monolayer. Langmuir. 2006; 22:9473–9476. [PubMed: 17073464]

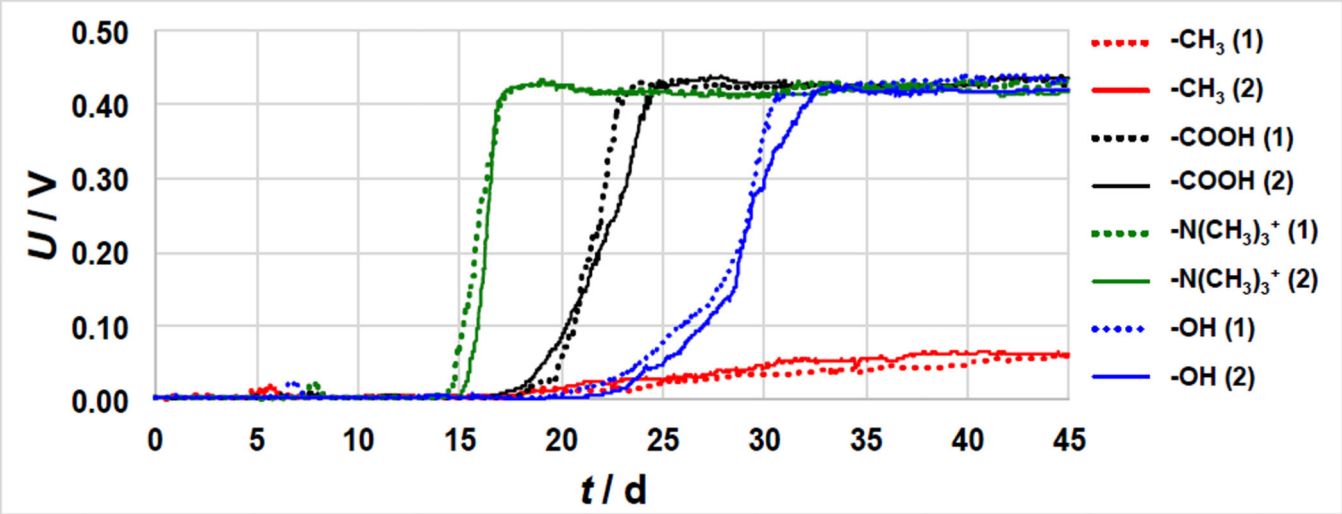

Figure 1.

Voltage trends of duplicate MFCs operated with different SAMs-modified gold anodes over 45 days of operation. The numbers in the brackets indicate the number of the replicate sample.

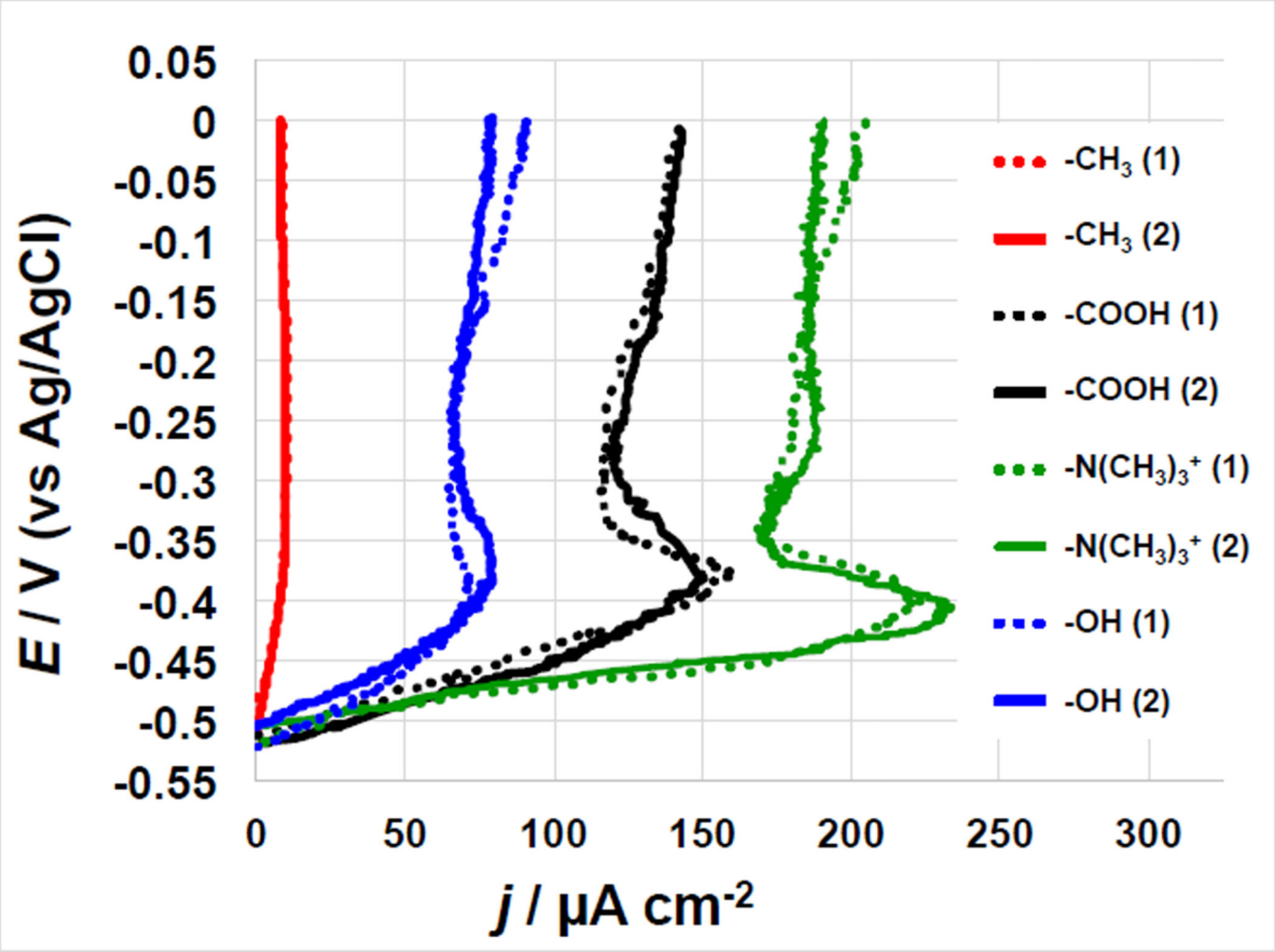

Figure 2.
Anode polarization curves for duplicate MFC systems featuring different SAMs-modified anodes after 45 days operations. The numbers in the brackets indicate the number of the replicate sample.

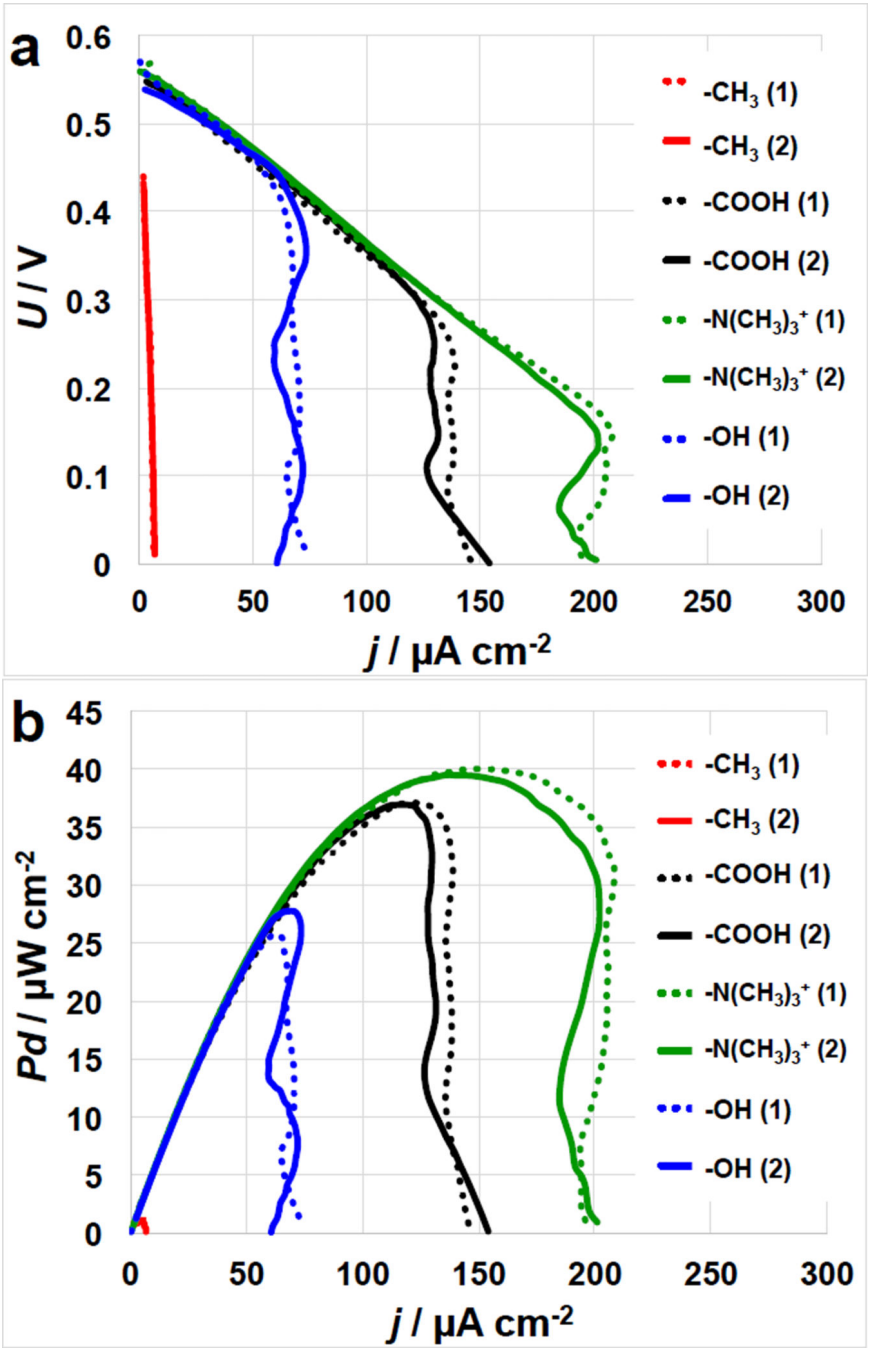

Figure 3.
Cell polarization (I-V) curves (a) and power curves (b) of MFCs with SAMs-modified anodes. The numbers in the brackets indicate the number of the replicate sample.

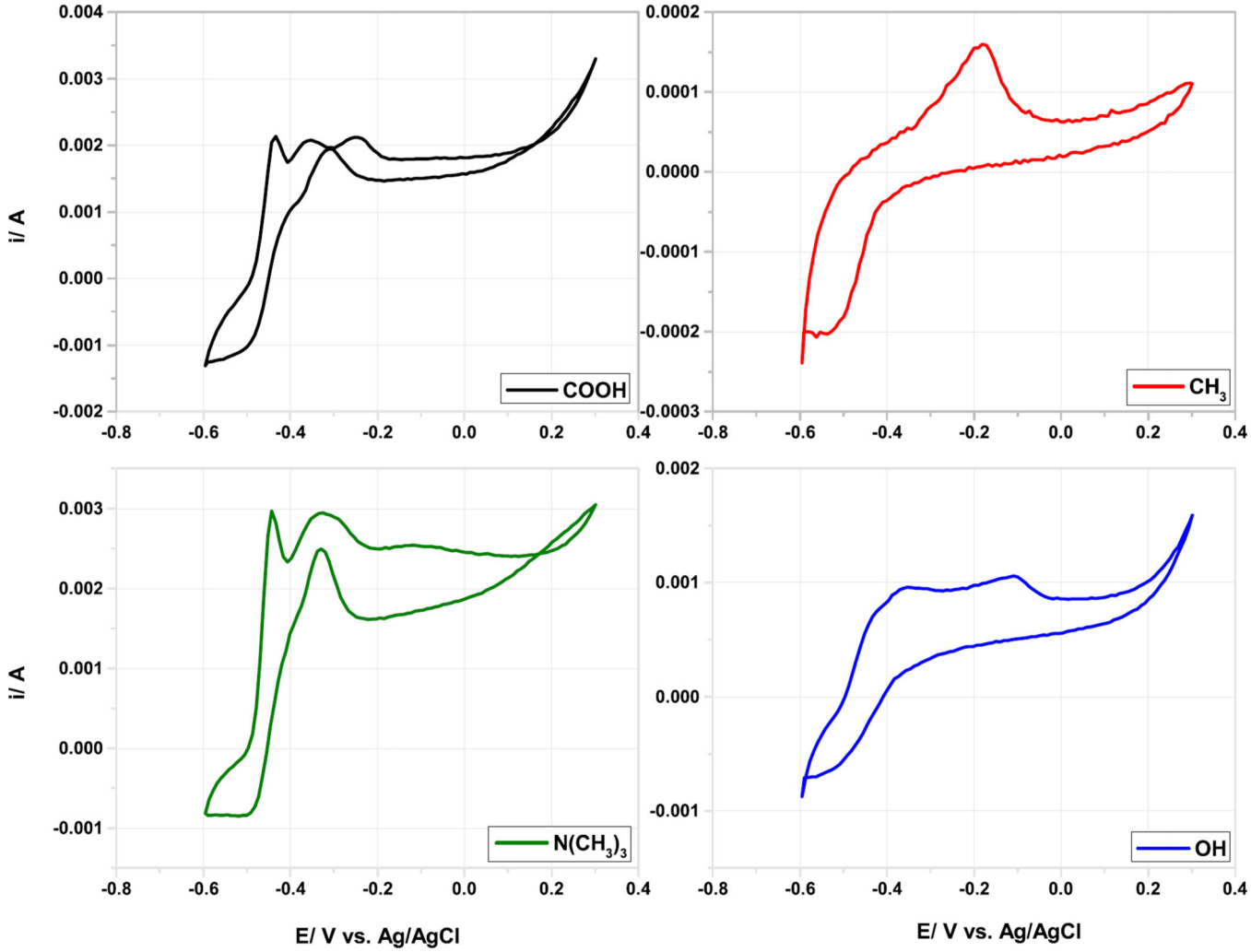

Figure 4.
Cyclic Voltammograms of the different modified anodes performed at scan rate of 2 mV s^{-1}.

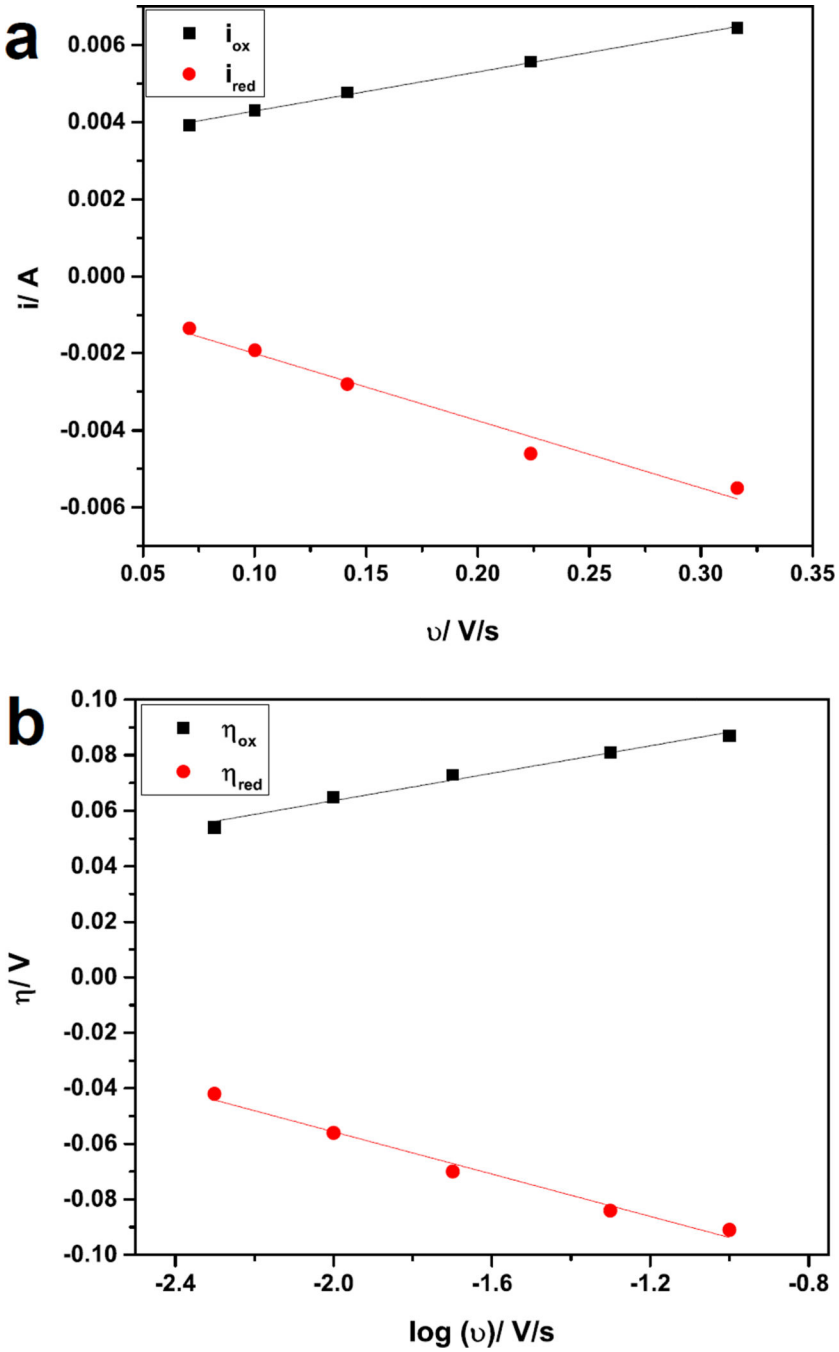

Figure 5.

Representative current-scan rate dependence graph (a) and Laviron plot (b) for $-N(CH_3)_3^+$ modified gold electrode.

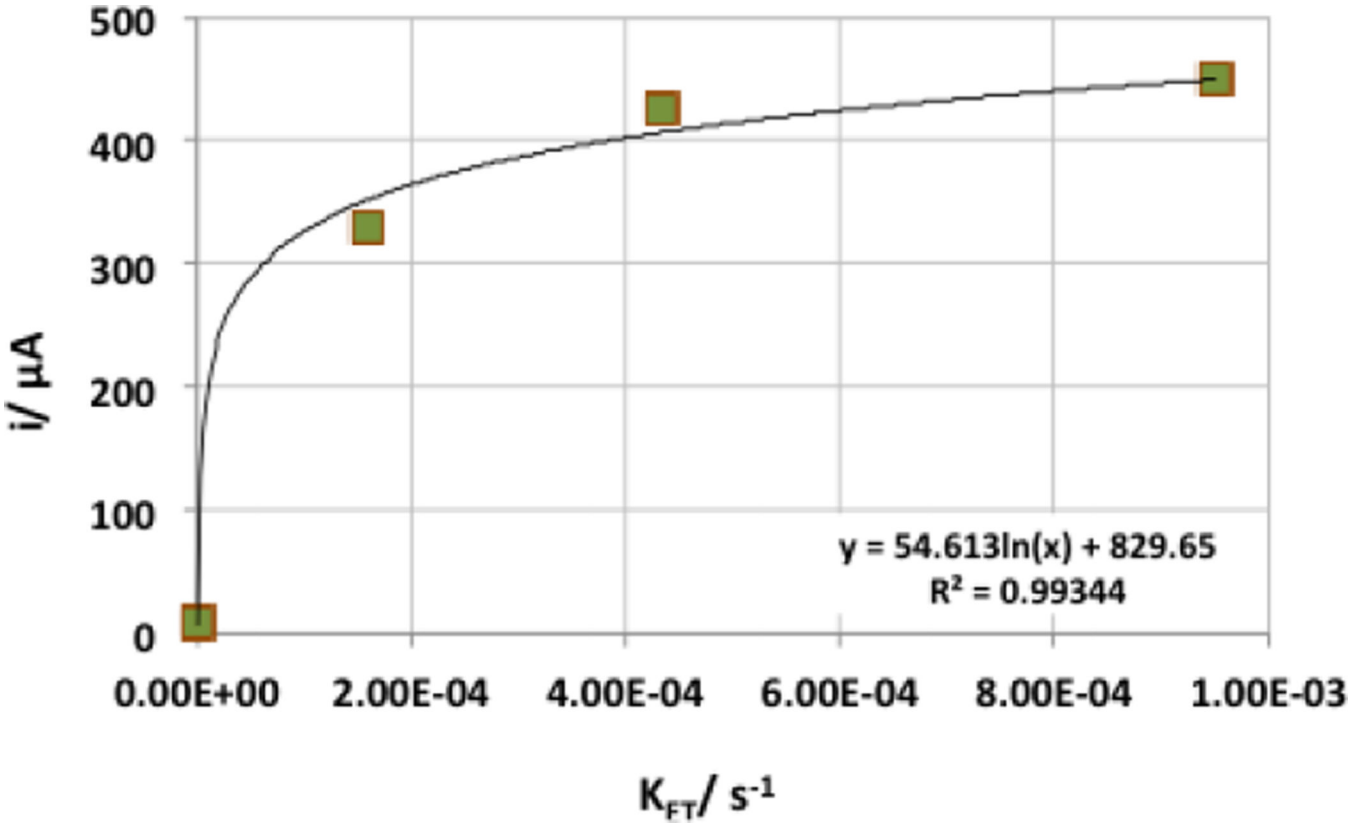

Figure 6.

Dependence of the current generated by the microbial anodes and the calculated electron transfer rate.

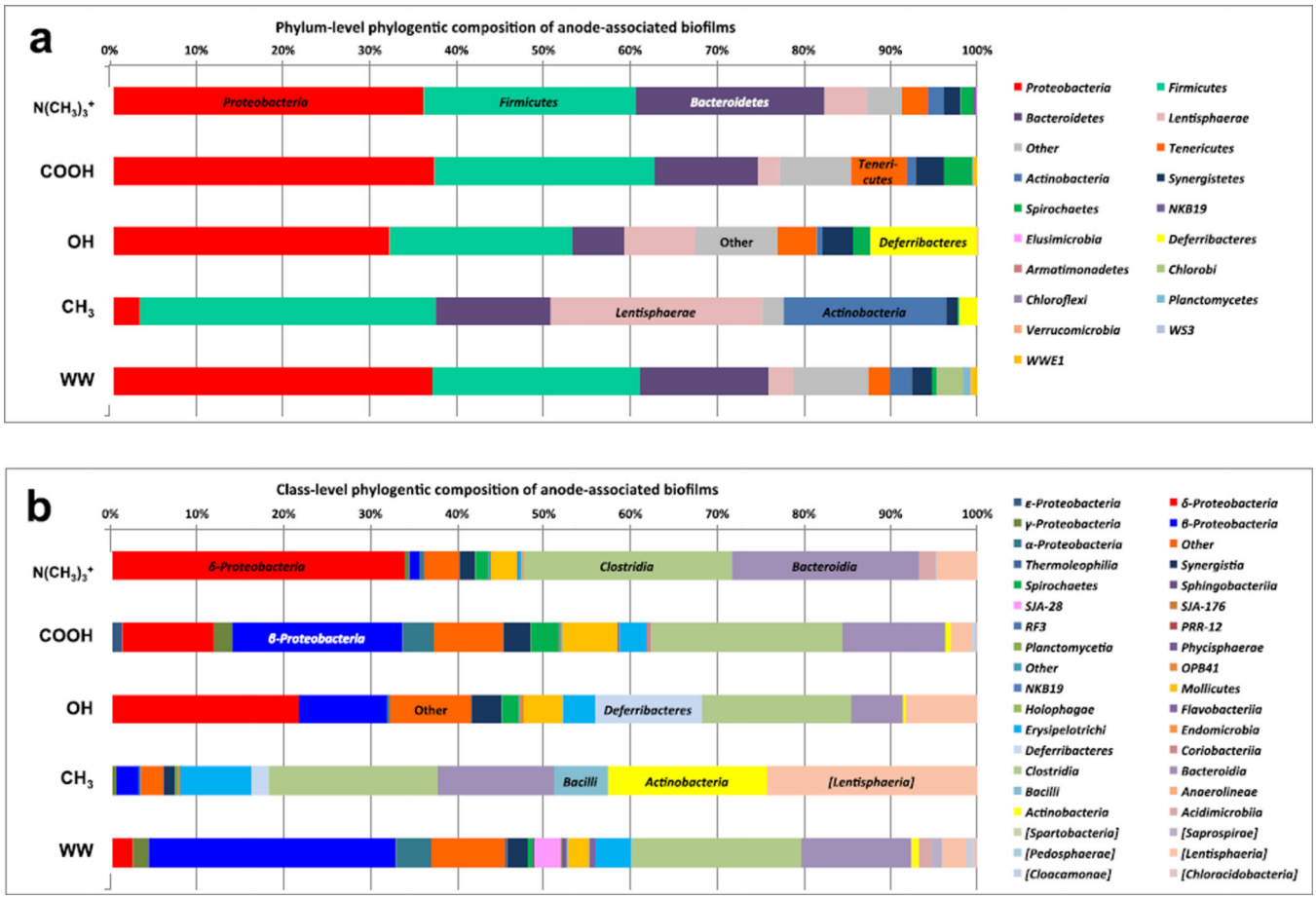

Figure 7.

Phylum-level taxonomic distribution of 16S rRNA community profile within anode electrochemically active bacteria (a) and class-level taxonomic profile of 16S rRNA community profile within anode electrochemically active bacteria (b).

Table 1

Electron transfer rate constant (K_{ET}) and formal redox potential of the redox reaction of the different anodic surfaces

	K_{ET}, s^{-1}	$E^{0'}$, V
$N(CH_3)_3^+$	$9.50*10^{-4}$	−0.468
COOH	$4.34*10^{-4}$	−0.468
OH	$1.58*10^{-4}$	−0.438
CH_3	$2.87*10^{-7}$	−0.348